Journal of Zhejiang University-SCIENCE B (Biomedicine & Biotechnology) in press
www.jzus.zju.edu.cn; www.springer.com/journal/11585
E-mail: jzus_b@zju.edu.cn

Research Article

https://doi.org/10.1631/jzus.B2500470

Human placental mesenchymal stem cells and derived exosomes alleviate oxidative stress and ferroptosis via the Nrf2/GPX4 pathway in hemorrhagic shock-induced acute lung injury

Shuai JIANG[1,2,3], Qin ZHANG[1,2], Ping WANG[1,2], Mengxiao FENG[1,2], Congying SONG[1,2], Yuanqiang LU[1,2]✉

[1]*Department of Emergency Medicine, The First Affiliated Hospital, School of Medicine, Zhejiang University, Hangzhou 310003, China*
[2]*Zhejiang Key Laboratory for Diagnosis and Treatment of Physic-chemical and Aging-related Injuries, Hangzhou 310003, China*
[3]*Department of Trauma Center and Traumatic Orthopedics, The Third Affiliated Hospital of Soochow University, Changzhou 213000, China*

Abstract: Hemorrhagic shock (HS) induces acute lung injury (ALI) in the early phase. Mesenchymal stem cells (MSCs) have shown potential in ameliorating HS-induced ALI; however, the mechanisms involved remain unclear. Our study investigated the therapeutic effects of human placental mesenchymal stem cells (hPMSCs) on HS-induced ALI and explored the underlying mechanisms. Male Sprague-Dawley (SD) rats were used to establish a model of HS, and the treatment group received injected hPMSCs. The biodistribution of hPMSCs in various organs of rats was imaged with the in vivo imaging system (IVIS) spectrum imaging system. The therapeutic effect and potential mechanisms for hPMSCs to improve HS-induced ALI were evaluated. The lungs and liver of HS rats were the main migration targets after hPMSCs transplantation. HPMSCs markedly mitigated lung pathological damage and diminished levels of reactive oxygen species (ROS), malondialdehyde (MDA), and Fe^{2+} in the lungs of HS rats, while also enhancing glutathione peroxidase 4 (GPX4) protein expression. Exosomes derived from hPMSCs were taken up by rat alveolar type Ⅱ epithelial (AT2) cells to inhibit ferroptosis by promoting overexpression of Nuclear factor erythroid 2-related factor 2 (Nrf2). Our study demonstrates the potential of hPMSC transplantation as a treatment for HS-induced ALI. The protective mechanism of hPMSCs for HS-induced ALI may include regulation of oxidative stress and ferroptosis.

Key words: Hemorrhagic shock; Acute lung injury; Mesenchymal stem cells; Exosome; Ferroptosis

1 Introduction

Hemorrhagic shock (HS) is the most common type of shock and a major contributor to mortality in surgical and trauma patients (Zhang et al., 2020). Previous research has demonstrated that the lungs are the first organs to sustain damage during HS (Wang et al., 2021). Acute lung injury (ALI) can develop into acute respiratory distress syndrome (ARDS), which is one of the main causes of death in patients with HS (He et al., 2021). The in-hospital mortality of ALI/ARDS patients is as high as 38%-46% (Villar et al., 2015; Zhou et al., 2019). In addition, 50%-70% of patients who survive ALI/ARDS continue to suffer from long-term physical and psychological disability (Herridge et al., 2011; Fan et al., 2014). The need for an effective means to treat ALI/ARDS caused by HS is clear.

✉ Yuanqiang LU luyuanqiang@zju.edu.cn
Yuanqiang LU, https://orcid.org/0000-0002-9057-4344
Shuai JIANG, https://orcid.org/0000-0001-7643-4639
Qin ZHANG, https://orcid.org/0009-0002-1968-3086
Ping WANG, https://orcid.org/0009-0008-5860-0072
Mengxiao FENG, https://orcid.org/0000-0002-1575-9613
Congying SONG, https://orcid.org/0000-0003-0822-0289

Received Aug. 8, 2025; Revision accepted Dec. 1, 2025;
Crosschecked xxx. xx, 20xx; Published online xxx. xx, 20xx

Mesenchymal stem cells (MSCs) are a class of multipotent stem cells with strong proliferative ability and differentiation potential, and are an important source of cell therapy in regenerative medicine (Fu et al., 2019). The potential therapeutic value of MSCs is that they can directly differentiate into various types of cells, secrete various cytokines and growth factors, regulate immunity, reduce inflammation, and promote the repair of damaged tissues (Barrachina et al., 2020). Exosomes derived from MSCs are extracellular vesicles measuring approximately 30 nm to 150 nm in diameter. They are abundant in cytokines, mRNA, and microRNAs, and play a crucial role in regulating the metabolic activity of cells and tissues (Mashouri et al., 2019). Studies have reported that MSC transplantation could markedly decrease pulmonary vascular permeability, improve endothelial function, and alleviate pulmonary edema and inflammation in HS rats or mice (Pati et al., 2011; Gore et al., 2016; Potter et al., 2018; Barry et al., 2022). Nonetheless, the migration pattern of MSCs in vivo post-transplantation and their distribution patterns in the main organs in HS animal models remain ambiguous. The potential mechanism of MSCs in therapeutic treatment of HS-induced ALI requires further investigation.

Deficiency of oxygen in the body due to HS is considered the primary factor leading to significant cellular and organ damage (Maier, 2014). The elevated levels of reactive oxygen species (ROS) induced by HS compromise the structural integrity of the pulmonary microvascular endothelium, resulting in disruption of the endothelial barrier and subsequent release of a substantial volume of protein-rich fluid (Tasoulis et al., 2009; Di et al., 2016). Consequently, HS-induced ALI is significantly associated with increased oxidative stress and aggravated mitochondrial damage (Wang, et al., 2021), indicating a robust link with the onset of ferroptosis (Stockwell, 2022). Ferroptosis is a form of cell death defined by the accumulation of lipid peroxides and increased levels of free iron. This concept was initially introduced by Dixon's team in 2012 (Dixon et al., 2012). Recent studies have demonstrated that ferroptosis contributes to the progression of multiple diseases and that inhibition of ferroptosis may result in anti-inflammatory effects, reduction of oxidative stress, and protection of vital organs (Bao et al., 2021; Wang et al., 2022). Nonetheless, it remains uncertain whether MSCs can ameliorate HS-induced ALI through regulation of oxidative stress and ferroptosis.

Nuclear factor erythroid 2-related factor 2 (Nrf2) is considered a crucial molecule in controlling levels of cellular oxidative stress and ferroptosis (Dodson et al., 2019b). Nrf2 and kelch-like ECH-associated protein 1 (Keap1) normally combine to create a complex in the cytoplasm (Leung et al., 2019). Upon activation, Nrf2 separates from Keap1 and binds to the promoter region of the antioxidant response element (ARE) to increase expression of glutathione peroxidase 4 (GPX4), thereby inhibiting ferroptosis (Dodson et al., 2019a). Thus, we hypothesized that MSC transplantation could improve HS-mediated ALI by reducing oxidative stress levels and inhibiting ferroptosis via Nrf2.

In this study, we aimed to investigate the efficacy of MSC transplantation in alleviating ALI in HS rats, to analyze the in vivo distribution characteristics of MSCs after transplantation, and to elucidate the potential mechanisms, thereby developing an innovative therapeutic strategy for HS-induced ALI.

2 Materials and methods

2.1 Preparation of MSCs

Human placental tissue was acquired from donors at the First Affiliated Hospital, College of Medicine, Zhejiang University, China. The protocol for handling human tissue and cells in this work was approved by the Research Ethics Committee of the First Affiliated Hospital (Reference No. 2013–272). Cultivation of human placental mesenchymal stem cells (hPMSCs) was performed as previously described (Cao et al., 2012). HPMSCs were cultured in a humidified incubator (Thermo Fisher, USA) at 37°C with 21% oxygen and 5% carbon dioxide in a specific medium (STEMCELL, Canada) within 25 cm² cell-culture flasks (Thermo Fisher, USA). We used hPMSCs from passages 3 to 5.

2.2 Identification of MSCs

HPMSCs were validated using flow cytometry: 5×10^5 cells were washed twice with PBS containing 0.5% (volume fraction, the same as below) bovine serum albumin (Sangon, China) and underwent incubation with

monoclonal antibodies for 30 min. The cells were treated in darkness at room temperature for 30 min with allophycocyanin-conjugated antibodies: CD73, CD90, CD105, CD19, CD34, and CD45 (1:50 (volume ratio, the same as below); eBioscience, USA), followed by washing with PBS. Isotype antibodies (1:50; eBioscience, USA) were employed as controls to mitigate nonspecific binding. Surface antigen expression was assessed with a BD LSR II flow cytometer (Becton Dickinson, USA). To assess the capacity for adipogenic and osteogenic differentiation, hPMSCs (passages 3–5) were seeded in 6-well multidishes (Nunc, Denmark) and cultivated in adipogenic and osteogenic medium (Cyagen Biosciences, China) according to the protocols.

2.3 Preparation of MSC exosomes

HPMSCs were cultivated in an exosome-free medium and subsequently extracted by ultracentrifugation. After 48 h, the conditioned medium derived from hPMSCs was harvested and then centrifuged at 2000 × g for 20 min to exclude debris and cells. The supernatant was obtained and deposited to a new sterile tube, then centrifuged at 10,000 × g for 15 min. The supernatant was subjected to filtration through a 0.22-μm-pore sterile filter, then subjected to ultracentrifugation at 110,000 × g for 70 min at 4 °C to isolate exosome pellets. The protein content of the concentrated exosomes was quantified with a BCA protein-assay kit (Thermo Fisher, USA).

2.4 Identification of MSC exosomes

Human placental mesenchymal stem-cell-derived exosomes (hPMSC-Exos) were identified by western blot analysis, focusing on the marker proteins Hsp70, CD63, and CD81. The morphology of hPMSC-Exos was examined using a 120 kV refrigerated transmission electron microscope (FEI Company, USA). We employed the ZETAVIEW particle potentiometric titration and particle size analyzer (Particle Metrix, Germany) to determine exosome-particle size distribution by means of nanoparticle tracking analysis (NTA).

2.5 HS rat experimental model and administration

Male Sprague-Dawley (SD) rats weighing 180–220 g and aged 7–9 weeks were acquired from the Laboratory Animal Centre of the Medical Institute of Zhejiang Province in Hangzhou, China. All experiments were conducted using protocols approved by the Animal Care Ethics Committee of the First Affiliated Hospital, Zhejiang University (Reference No. 2023-84). Prior to the experiments, all rats were maintained with a 12 h light and 12 h dark cycle for one week in an environment with controlled temperature and humidity. They were fed with food and water under specific pathogen-free (SPF) conditions. HS operation was consistent with our previous research but with minor modifications (Yao et al., 2017). A diluted heparin solution (100 U/mL) was used to rinse the syringes and pipelines to prevent clotting. HS rats went through three stages: (i) Blood loss: The amount of blood to be drawn was calculated according to the rat's body weight (g), 2 mL/100g for the first 10 min and 1 mL/100 g for the next 10 min; the drawn blood was kept in the syringe before being reinfused; (ii) Maintenance: A 40-min shock maintenance stage was entered after the end of the bleeding stage, during which no transfusion or bloodletting was performed; (iii) Transfusion: The blood drawn was uniformly returned to the rats through the left femoral vein within 30 min. The sham group underwent the same surgical procedures but without bleeding and resuscitation, and was sampled at the same time point. Rats were anesthetized via intraperitoneal injection of ketamine (75 mg/kg; Sigma, USA) and xylazine (10 mg/kg; Sigma, USA). At 24 h or 72 h after model establishment, we euthanized the rats with pentobarbital sodium (100 mg/kg, Sigma, USA) for tissue collection.

Rats in the HS+hPMSC group received a tail-vein injection of 5×10^6 hPMSCs resuspended in 200 μL PBS after HS, while the HS+PBS group received only 200 μL PBS. Rats in the dimethyl sulfoxide group received only 2% DMSO as vehicle control (DMSO, Sigma, USA). ML385 (S8790, Selleck, USA), a specific inhibitor of Nrf2, was diluted with 5% DMSO. Rats in the HS+hPMSC-Exos+ML385 group were injected with ML385 (30 mg/kg) two hours before the HS operation.

2.6 Cell culture and treatment

Primary alveolar type Ⅱ epithelial (AT2) rat cells (Procell, China) were cultivated in complete culture medium (Procell, China). We cultured them in a humidified incubator (Thermo Fisher, USA) at 37℃ with 21% O_2 and 5% CO_2. To create an in vitro model of ferroptosis in AT2 cells, 1×10^5 AT2 cells were exposed to RAS-selective lethal 3 (RSL3), a small-molecule compound that induces ferroptosis through inactivation of GPX4 (Wang et al., 2024). AT2 Cells were divided into three groups: the Control group; the RSL3 group, treated with RSL3 (0.2 μM, Selleck, USA) for 24 h; and the RSL3+hPMSC-Exos group, cocultured with RSL3 (0.2 μM) and hPMSC-Exos (from 0.5 μg/mL to 1.5 μg/mL) for 24 h.

2.7 MSC labeling and tracking in rats

We labelled the isolated hPMSCs with 5 μM 1,1’-dioctadecyl-3,3,3’,3’-tetramethylindotricarbocyanine iodine (DiR, Thermo Fisher, USA). Labelled hPMSCs were administered through the tail vein to both the sham and HS groups. At 24 h or 72 h post injection, the rats were euthanized and their organs harvested and imaged on an IVIS Spectrum (PerkinElmer, USA). We chose excitation and emission filters at 750 nm and 800 nm to detect fluorescence.

2.8 Staining of HPMSC-Exos with PKH67

The isolated exosomes were combined with the prepared 2 × dye solution in 1 mL of Diluent C and incubated for 4 min in the dark. After PBS washing, hPMSC-Exos underwent ultracentrifugation at 110,000 × g at 4°C for 1 h. Subsequently, the exosomes were tagged with PKH67 (PKH67GL; Sigma, USA) and resuspended in PBS.

2.9 Hematoxylin–eosin staining

Lung tissues were fixed for 24 h in 4% paraformaldehyde (Servicebio, China) and embedded in paraffin, then sectioned into 5 μm-thick slices. Next, different concentrations of ethanol were used for rehydration. The slices were then washed three times (5 min each) with distilled water. Finally, the slices were stained with hematoxylin and eosin (H&E) solution (Servicebio, China).

2.10 Immunofluorescence staining

The immunofluorescence assay was used to assess ROS levels in rat lung tissue. Fresh-frozen lung samples were sectioned continuously to a thickness of 4 μm and maintained at room temperature. The frozen slides were treated with an ROS staining solution (1:500; Sigma, Germany) at 37 °C for 30 min. Following three washes, the slides were incubated with 4',6-Diamidino-2'-phenylindole (DAPI, Servicebio, China) for 10 min. The tissue sections were examined under a microscope, and images were captured using fluorescence microscopy.

2.11 Transmission electron microscopy

The rat lung-tissue slices (about 3 mm^3 in size) were preserved in 2.5% glutaraldehyde at 4℃ overnight, and treated with 1% osmium acid for 1 h. Then, the fixed tissues underwent dehydration with graded ethanol and acetone before being embedded in epoxy resin. Ultrathin sections were prepared using an ultramicrotome and analyzed with a transmission electron microscope (TEM).

2.12 Western blot

We isolated and standardized total proteins from the lung tissue samples with a BCA protein assay kit (Beyotime, China). The 12% SDS-PAGE gels (Bio-Rad) were used to separate protein extracts, which were subsequently transferred to polyvinylidene difluoride membranes (Merck, Germany). Following a 1-hour incubation at room temperature with 5% skim milk for blocking, the membranes were treated with primary antibodies: Nrf2 (1:1000, Abcam, USA), GPX4 (1:1000, Abcam, USA), Hsp70 (1:1000, Abcam, USA), anti-CD63 (1:1000, Abcam, USA), anti-CD81 (1:1000, Abcam, USA), beta actin (1:500, Proteintech, USA), beta tubulin (1:2000, Proteintech, USA), alpha tubulin (1:5000, Proteintech, USA), and goat anti-rabbit IgG

H&L (HRP) (1:5000, Abcam, USA).

2.13 Visualization of oxidative stress

AT2 cells from each group were resuspended in 500 μL of PBS with C11-BODIPY581/591 (2.5 μM, ABclonal, China) and incubated for 30 min. The cell membrane and cell nuclei were stained with 1,1′-dioctadecyl-3,3,3′,3′-tetramethylindocarbocyanine perchlorate (Dil, Invitrogen, USA) and Hoechst (Beyotime, China), respectively. The cells were then washed twice with PBS and examined using laser confocal microscopy.

2.14 Iron measurements

The harvested lung-tissue slices were homogenized with PBS, and after centrifugation, the supernatant was collected. We measured the concentration of free ferrous ions (Fe^{2+}) using an iron assay kit (Abcam, USA) in accordance with the manufacturer's instructions.

2.15 Statistical Analysis

The data are presented as the mean±standard deviation. We conducted statistical analyses using GraphPad Prism 8.0.1 (GraphPad Software Inc., USA), and assessed statistical significance via two-tailed unpaired Student's t-tests or one-way ANOVA, as appropriate. The data is defined as not significant (ns); $*P < 0.05$; $**P < 0.01$; $***P < 0.001$. All images are representative of at least three independent experiments.

3 Results

3.1 ALI occurred in the early stage of HS

Fig. 1a illustrated the procedure for establishing this experimental animal model. Rats in the HS group were subjected to blood loss, maintenance, and transfusion. The rats were euthanized 24 h and 72 h post model establishment, and lung tissues were subsequently collected. All rats in each group survived within 72 h of model establishment. The sham group showed minimal fluctuations in mean arterial pressure (MAP), with an average of 91.50±10.28mmHg throughout the entire period. In contrast, the rats in the HS group experienced a sharp decrease in MAP during the bleeding stage, with a mean of 24.67±5.47mmHg. Subsequently, MAP slowly increased to 43.67±7.20mmHg during the maintenance stage and further increased to 106.50±12.47mmHg during the transfusion stage (Fig. 1b). The lung surface of the sham group had a smooth and pale pink appearance with a full shape, but the lung surface of the HS group rats displayed obvious congestion, a dark red color, and noticeable collapse (Fig. 1c). In addition, H&E staining revealed that, when compared to the sham group, the alveolar structure was damaged and the pulmonary septum was markedly expanded at 24h and 72 h following HS modeling. There was also an increase in capillary dilation and hemorrhage (indicated by the red arrow), as well as an elevated presence of inflammatory cells (indicated by the black arrow). Histological analysis confirmed the presence of lung injury in these rats 24 h and 72 h after simulation of hemorrhagic shock.

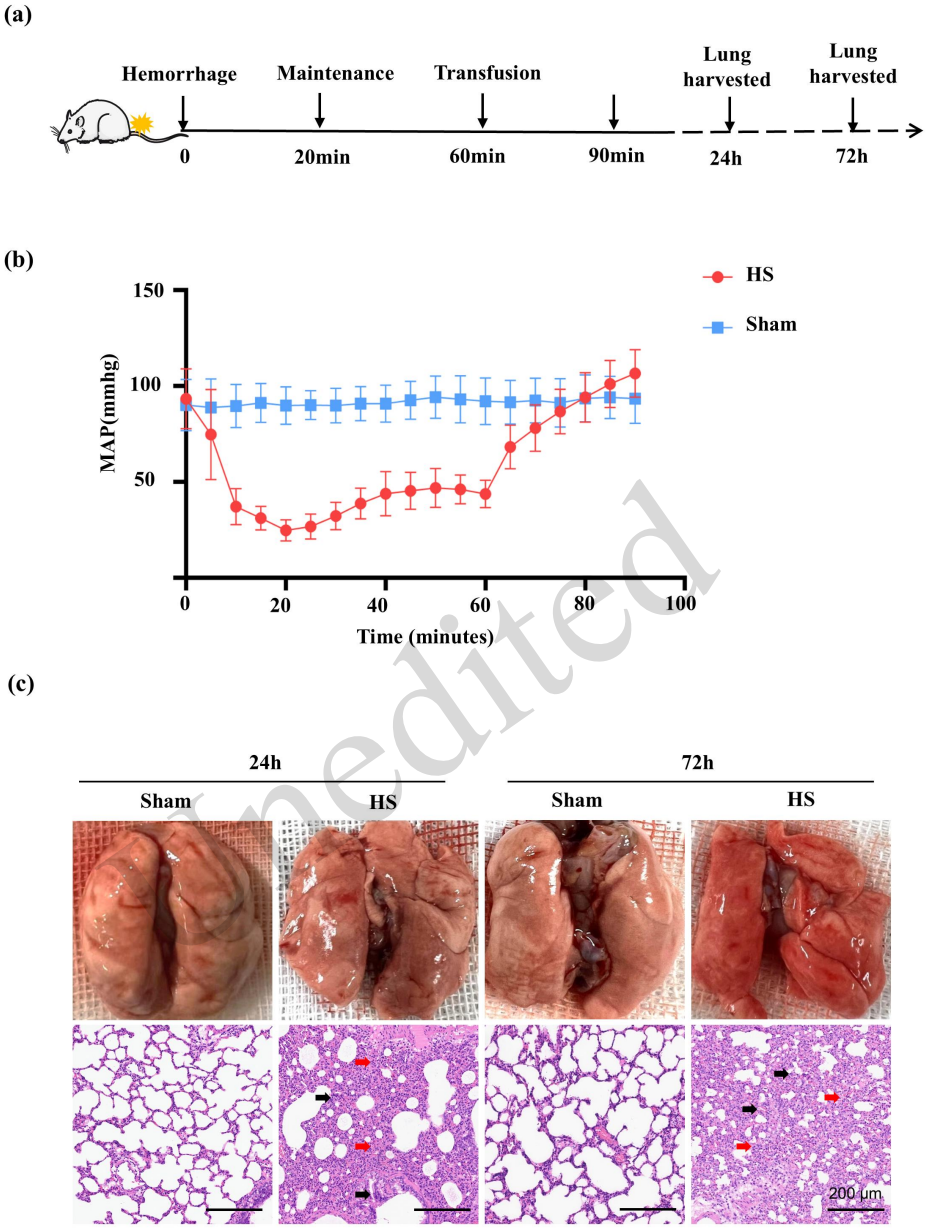

Fig. 1 HS leads to ALI in the early stage. (a) HS rat-model establishment and lung-tissue-sampling time-point diagram. (b) MAP values of Sham and HS rats during modeling (n=5 or n=6). (c) Representative gross view and H&E stained images of rat lungs from Sham and HS groups. Data are expressed as mean±SD. HS: hemorrhagic shock; ALI: acute lung injury; MAP: mean arterial pressure; H&E: hematoxylin and eosin. SD: standard deviation.

3.2 Therapeutic effect of hPMSCs on ALI in HS Rats

First, we identified the extracted hPMSCs. We observed the cell morphology via microscope (Fig. 2a). The capacity of cells for osteogenic differentiation (Fig 2b) and lipogenic differentiation (Fig. 2c), as well as the identity of surface markers (CD73, CD90, CD105, CD19, CD34, CD45), were confirmed by flow cytometry (Fig. 2d).

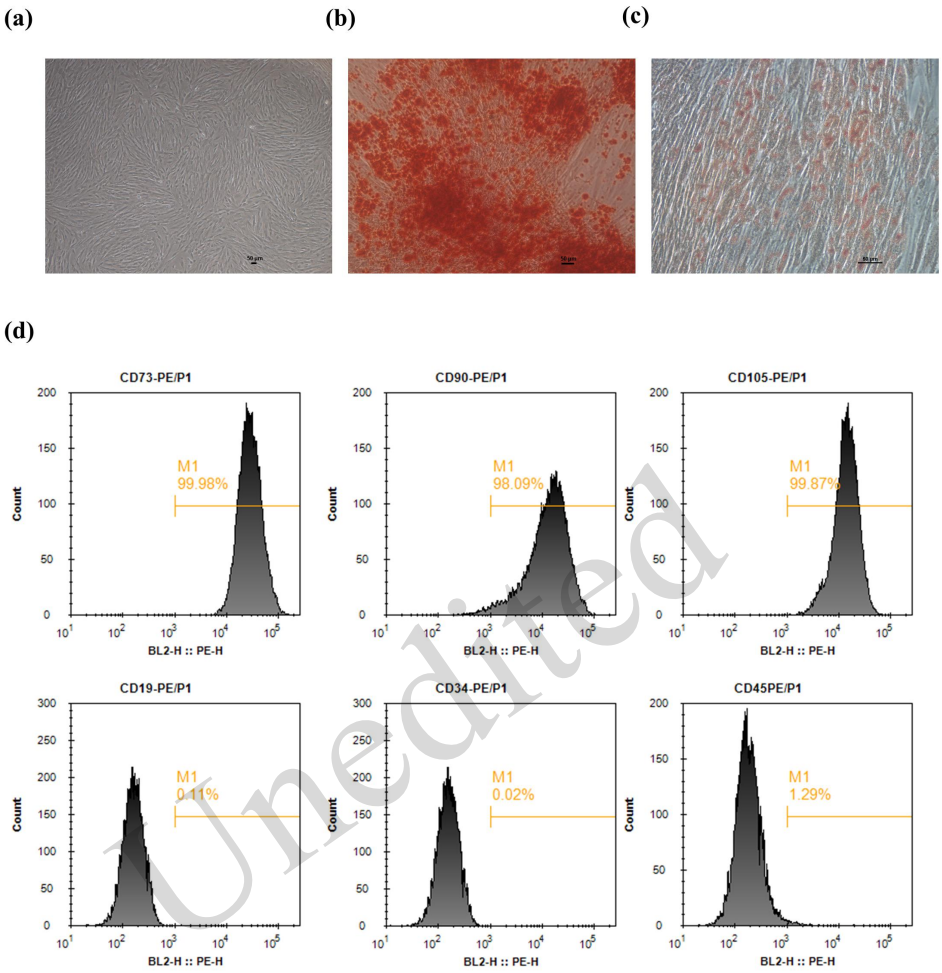

Fig. 2 Identification of hPMSCs. (a) Representative optical micrograph of hPMSCs. (b) Alizarin Red S and (c) Oil Red O staining of hPMSCs. (c) Flow cytometry analysis of MSC-associated surface markers (CD73, CD90, CD105, CD19, CD34, CD45). HPMSCs: human placental mesenchymal stem cells.

To explore the biodistribution of hPMSCs after transplantation, we injected DiR-labeled hPMSCs into rats through the tail vein, and visualized them with an IVIS imaging system (Fig. 3a). The fluorescence intensity of hPMSCs in the heart, liver, spleen, lung, kidney, and small intestine of rats in each group was detected. In the sham group, hPMSCs primarily accumulated in the lungs at 24 h or 72 h after transplantation, but at 72 h, they showed a notable decrease (Fig. 3b). Similarly, hPMSCs in the HS group were predominantly found in the lungs 24 h post-transplantation. At 72 h, the fluorescence-intensity ratio of hPMSCs in the liver of HS rats exhibited a significant increase, and a limited quantity of hPMSCs was identified in the lungs, kidneys, and small intestine (Fig. 3b). Interestingly, fluorescence quantification showed that the HS group had a lower number of hPMSCs in the lungs than did the sham group, at both 24 h and 72 h ($P < 0.05$). The fluorescence intensity of the HS group significantly dropped after hPMSC injection between 24 h and 72 h ($P < 0.05$) (Fig. 3c). We were also able to detect the remedial effect of hPMSCs on HS-induced ALI. The lungs of rats in the HS group exhibited a higher level of congestion and swelling compared to those in the HS + hPMSC group (Fig. 3d). H&E staining was conducted to assess histological alterations in the lung tissues. In comparison to the sham group, the HS group exhibited structural damage characterized by thickening of the alveolar walls, alveolar hemorrhage, and infiltration of inflammatory cells within the alveolar septum. However, administration of hPMSCs resulted in a

significant reduction of ALI in HS rats, as described below. (Fig. 3d).

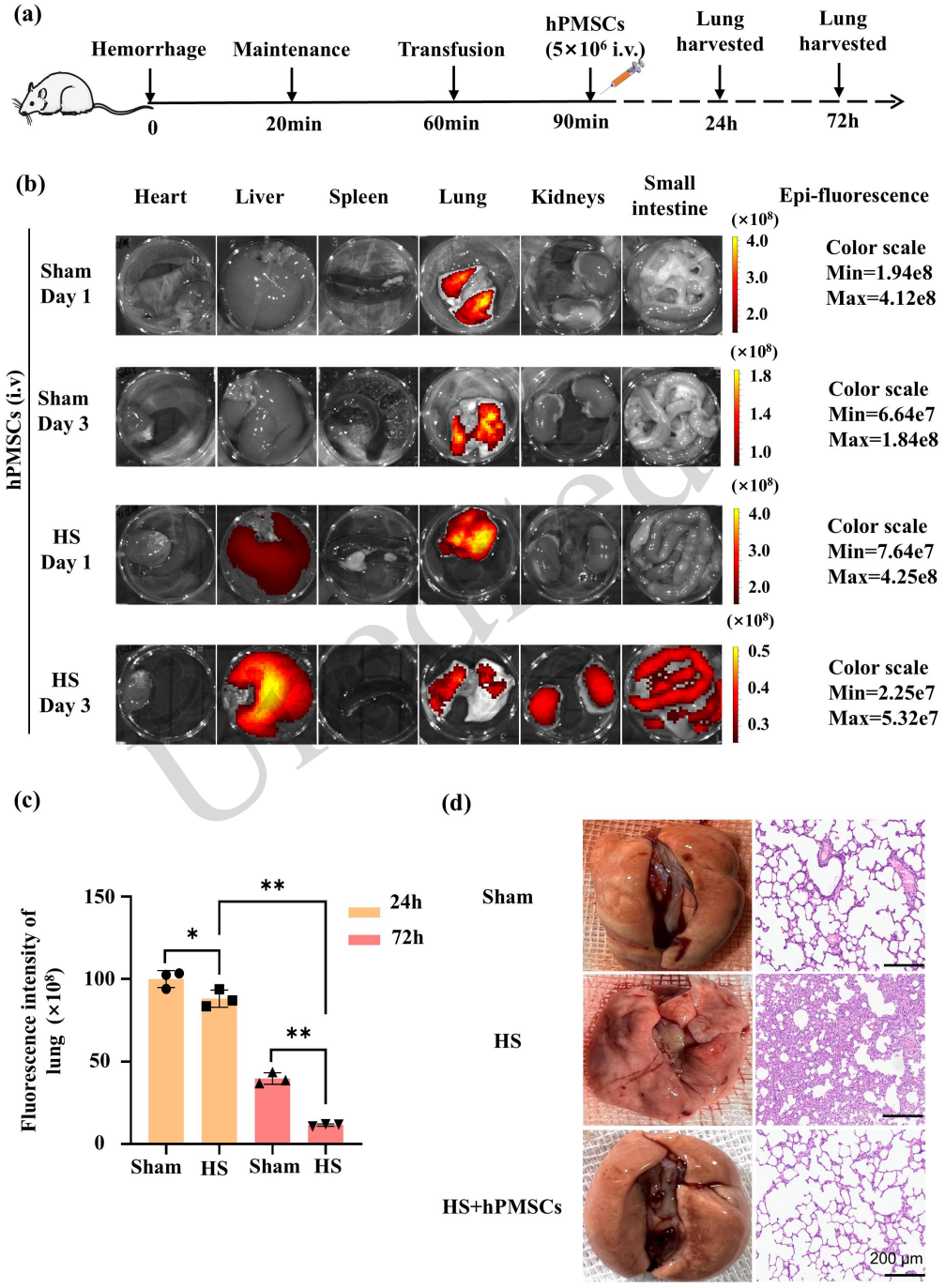

Fig. 3 Real-time Ex vivo imaging of hPMSCs in lungs of HS and Sham rats. (a) DiR-labeled hPMSCs were injected after the HS modeling operation, and lung tissue was harvested for real-time fluorescence imaging at 24h and 72h. (b) Ex vivo fluorescence biodistribution of hPMSCs in vital organs from both groups at 24 h and 72 h post injection. (c) Fluorescence intensity changes of hPMSCs in lung tissue from both groups at selected time points (n=3). (d) Representative micrographs for H&E staining of lung sections at 72h after hPMSC transplantation. Administration of hPMSCs largely prevented histopathologic alterations after HS injury. Data are expressed as mean ± SD, *P<0.05, **P<0.01. HPMSCs: human placental mesenchymal stem cells; HS: hemorrhagic shock; H&E: hematoxylin and eosin; SD: standard deviation.

3.3 Inhibitory effect of hPMSCs on ferroptosis in HS-induced ALI

To investigate the potential mechanism by which hPMSCs alleviate HS-induced ALI, we assessed expression of molecules related to oxidative stress and ferroptosis. As shown in Figs. 4a-4c, hPMSC treatment significantly reduced ROS, malondialdehyde (MDA), and Fe^{2+} to lower levels than those in the HS group at 72h. The mitochondrial morphology of AT2 cells in the HS+hPMSC group was superior to that in the HS group, indicating that hPMSCs may inhibit ferroptosis in AT2 cells (Fig. 4d). We further examined the effects of hPMSCs on GPX4 protein expression in rat lungs by western blot. Rats in the HS + hPMSCs group had higher GPX4 expression than HS rats, which further suggested that hPMSCs inhibited HS-induced ferroptosis (Figs. 4e-4f).

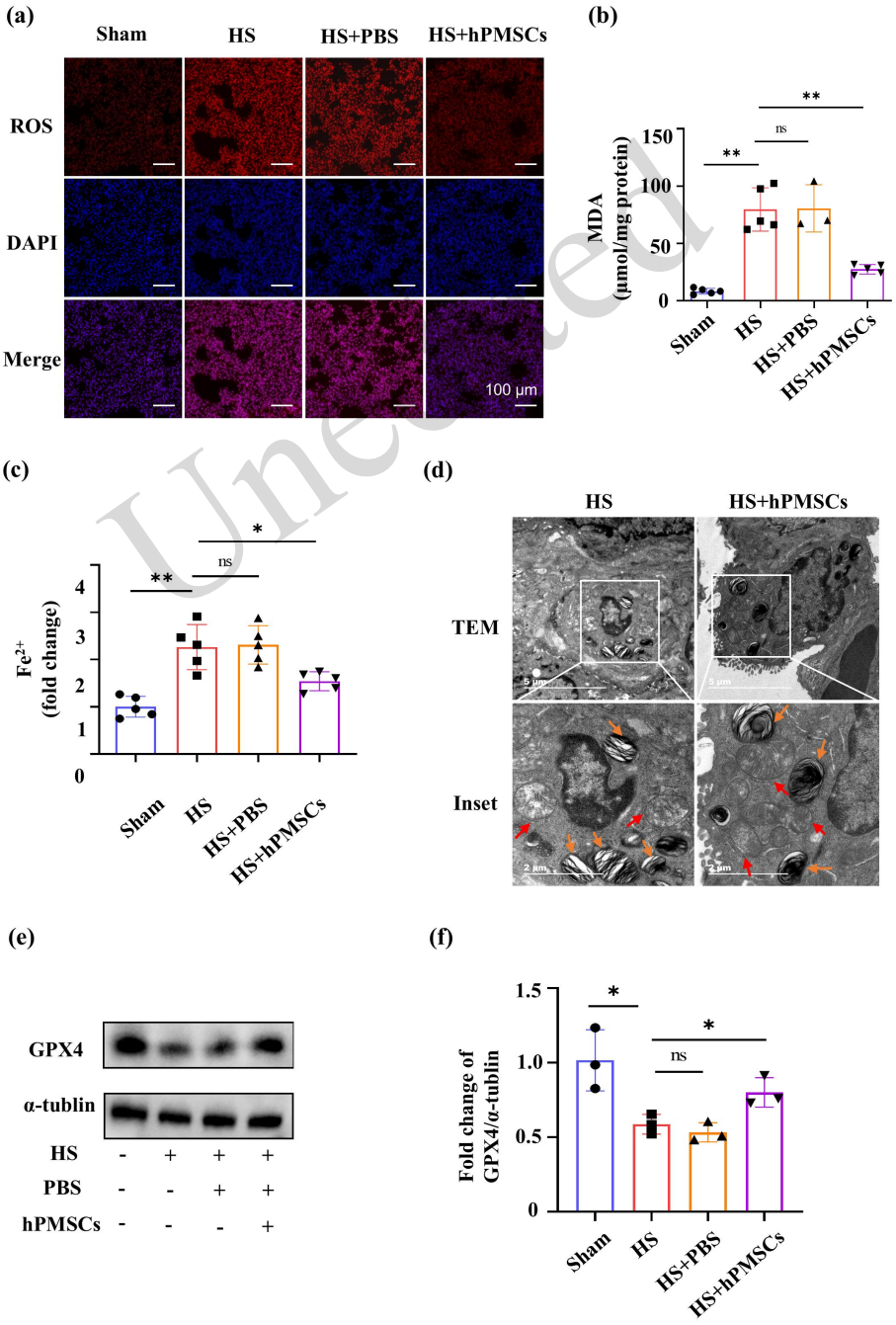

Fig. 4 HPMSCs attenuated oxidative stress levels and ferroptosis of lungs in HS-induced ALI. (a) Immunofluorescence micrographs of ROS expression (Red) of rat lungs obtained from Sham, HS, HS+PBS and HS+hPMSC groups at 72 h after injection. (b) MDA contents of HS rats treated with or without hPMSCs for 72 h (*n*=3 or *n*=5). (c) The Fe^{2+} concentration in rat lungs was measured (*n*=5). (d) TEM showing that outer mitochondrial membrane rupture in HS rat lungs was repaired by hPMSCs after injection at 72 h. Yellow arrows indicate the lamellar body of AT2 cells, and red arrows indicate mitochondria. (e) Protein expression for GPX4 in rat lungs obtained from each group (*n*=3). (f) Quantitative analysis of western blot. Data are expressed as mean±SD, **P*<0.05, ***P*<0.01. HPMSCs: human placental mesenchymal stem cells; HS: hemorrhagic shock; ROS: reactive oxygen species; PBS: phosphate-buffered saline; MDA: malondialdehyde; AT2: alveolar type II epithelial; GPX4: glutathione peroxidase 4; SD: standard deviation.

3.4 Uptake of hPMSC-Exos by RSL3-treated AT2 cells in vitro

Subsequently, we extracted exosomes from the hPMSC culture medium via ultracentrifugation. hPMSC-Exos were identified by western blot, TEM and NTA. These tests showed the existence of vesicles of 30-100 nm in size, which displayed similar characteristics to exosomes (Fig. 5a). Furthermore, surface markers of exosomes, such as Hsp70, CD63, and CD81, were present (Fig. 5b). NTA analysis demonstrated that approximately 98.1% of the particles had a diameter of around 120 nm (Fig. 5c). These results confirmed that we had successfully extracted hPMSC-Exos.

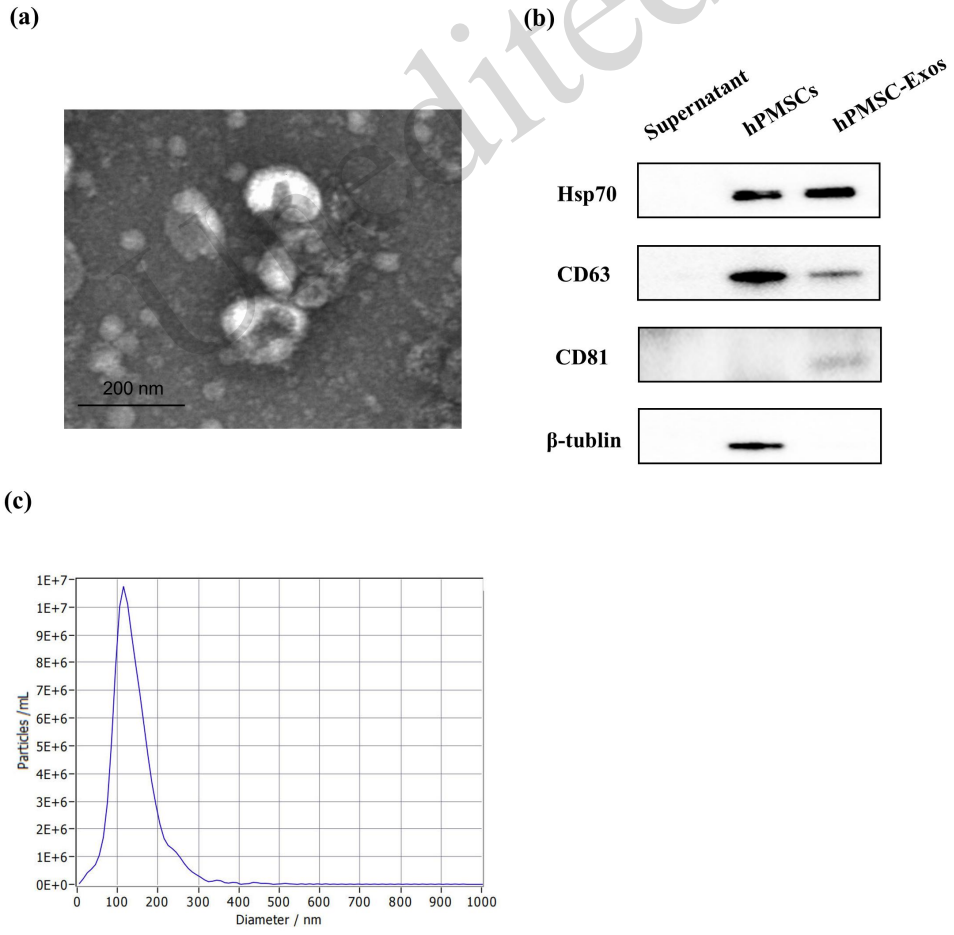

Fig. 5 Identification of hPMSC-Exos. (a) Expression of hPMSC-Exos surface markers Hsp70, CD63, and CD81 was detected by western blot. (b) hPMSC-Exo morphology under TEM observation; (c) NTA analysis of hPMSC-Exos particle size and concentration. HPMSC-Exos: human placental mesenchymal stem-cell-derived exosomes; Hsp70: Heat Shock Protein 70; TEM: transmission electron microscope; NTA: nanoparticle tracking analysis.

To determine whether AT2 cells could internalize hPMSC-Exos, we marked hPMSC-Exos with a green lipophilic fluorescent dye and co-cultured them with RSL3-treated AT2 cells for 24 h. The AT2 cells demonstrated significant uptake efficiency, as evidenced by the intense fluorescent green signal (Fig. 6a).

Following this, we assessed the levels of ROS and lipid peroxides in AT2 cells in the different groups. As shown in Figs. 6b-6c, treatment with RSL3 (a GPX4 inhibitor) resulted in a notable increase in ROS and lipid peroxidation levels, while treatment with hPMSC-Exos correspondingly reduced both ROS and lipid peroxidation levels. To investigate the potential mechanism, we examined the dose-dependent effects of hPMSC-Exo treatment on Keap1 and Nrf2 protein expression. Fig. 6d indicted that the Keap1 protein level was significantly downregulated, while the Nrf2 protein level was significantly upregulated. These results indicated that hPMSC-Exos reduced the levels of ROS and lipid peroxides in RSL3-treated AT2 cells in vitro and were associated with activation of Nrf2.

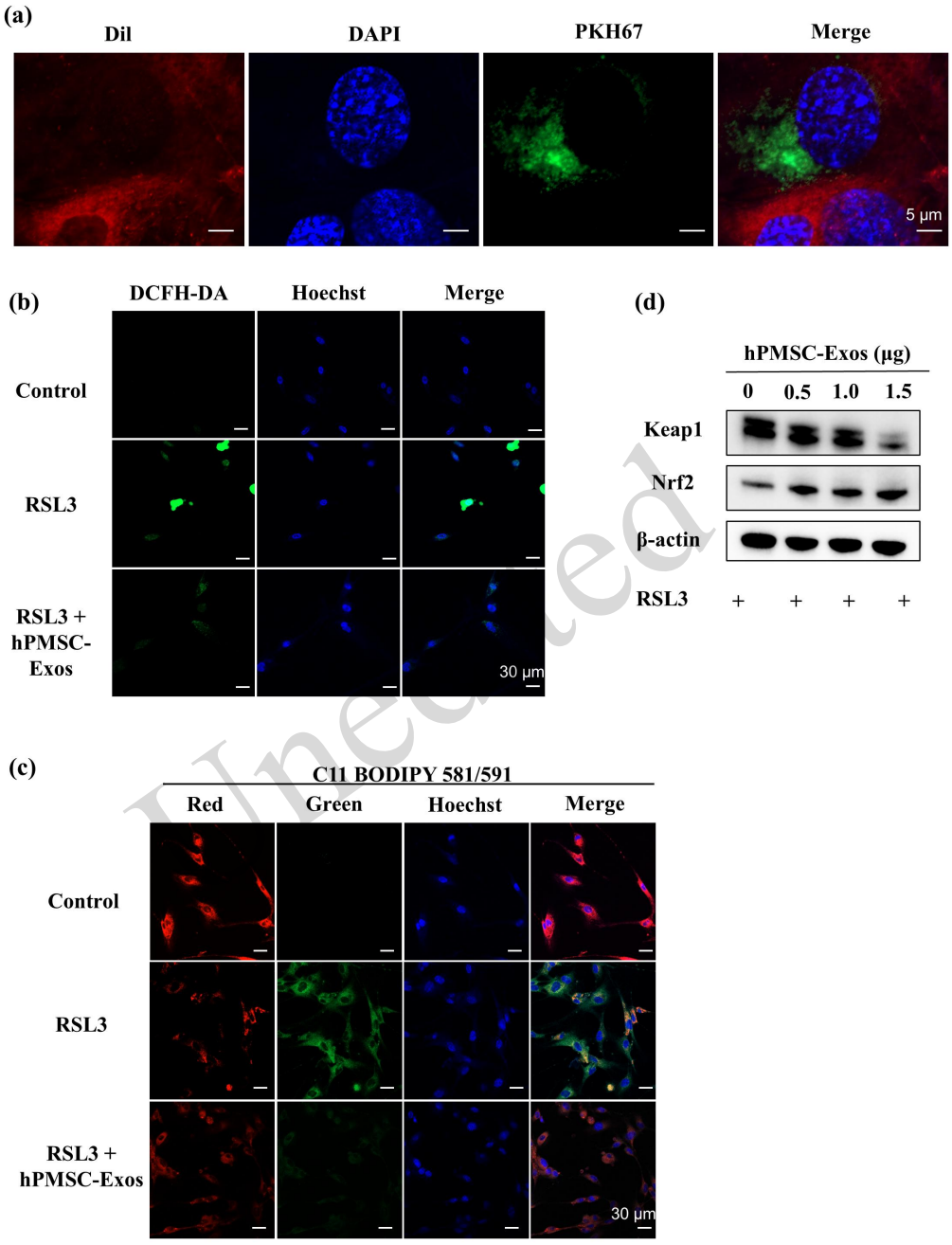

Fig. 6 HPMSC-Exos were endocytosed by AT2 cells and reduced oxidative stress levels in vitro. (a) Exosomes collected from hPMSC-conditioned medium were labeled with PKH67 and incubated with RSL3-treated rat primary AT2 cells for 24 h. The cell membrane was stained with Dil. The cell nuclei were stained with DAPI. PKH67 lipid dye was detected in AT2 cells treated with PKH67-labeled exosomes. Primary AT2 cells treated with control (PBS), 0.2 μM RSL3, or 0.2 μM RSL3 co-cultured with hPMSC-Exos (0.5 μg/mL). (b) ROS and (c) lipid peroxidation levels were measured by DCFH-DA and C11-BODIPY581/591 respectively, via laser scanning confocal microscope. (d) Keap1, Nrf2 protein levels in RSL3-treated AT2 cells co-cultured with 0, 0.5, 1, and 1.5 μg hPMSC-Exos were detected by western blot. HPMSC-Exos: human placental mesenchymal stem-cell-derived exosomes; DAPI: 4',6-Diamidino-2'-phenylindole AT2: alveolar type II epithelial; PBS: phosphate-buffered saline; RSL3: RAS-selective lethal 3; ROS: reactive oxygen species; Keap1: kelch-like ECH-associated protein 1; Nrf2: Nuclear factor erythroid 2-related factor 2.

3.5 Underlying mechanism of hPMSC-Exos-Mediated Ferroptosis inhibition in HS-induced ALI

Based on the in vitro efficacy of hPMSC-Exos, we examined their impact on HS-induced ALI in vivo. As shown in Fig. 7a, rats in the HS+Exo group received 100 μg of hPMSC-Exos following HS, while rats in the HS+Exo+ML385 group were injected with ML385 (a Nrf2 inhibitor) intraperitoneally 2 h prior to modeling. Interestingly, consistent with the protective effects of MSCs in vivo, hPMSC-Exos also ameliorated pathological injury in lung tissue and reduced the level of ROS in HS-induced ALI (Figs. 7b-7c). However, the protective effects of hPMSC-Exos in HS-induced ALI were abolished by ML385. Western blot analysis also indicated that hPMSC-Exos markedly elevated the protein levels of Nrf2/GPX4 in the lungs of HS rats, whereas ML385 pretreatment notably diminished this effect (Figs 7d-7f). These findings indicate that hPMSCs may activate the Nrf2/GPX4 signaling pathway via exosomes, thereby inhibiting ferroptosis in AT2 cells and improving HS-induced ALI.

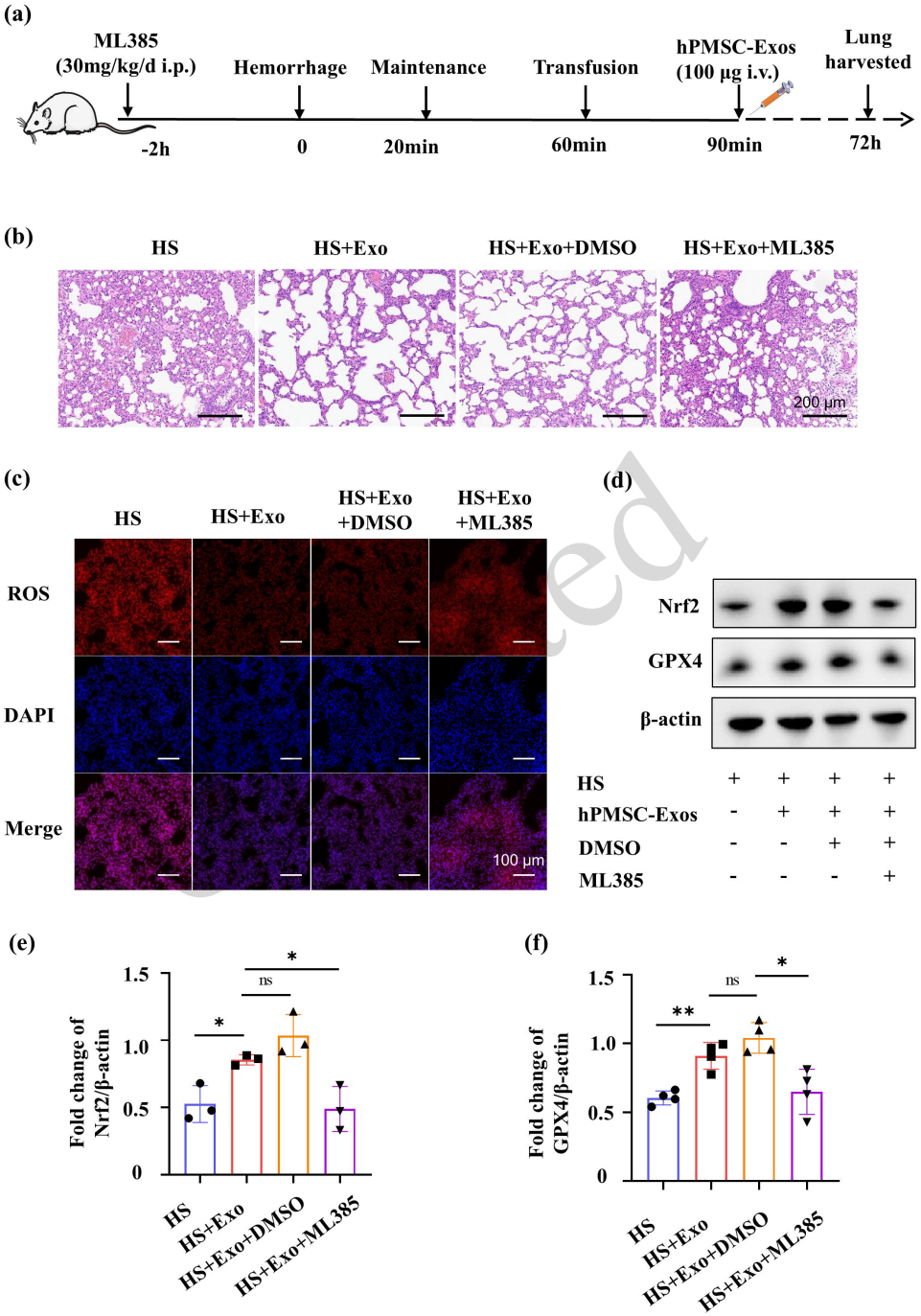

Fig. 7 hPMSC-Exos improved HS-induced ALI by inhibiting ferroptosis via the Nrf2/GPX4 pathway (a) The time points for HS rats with ML385 pretreatment, hPMSC-Exos injection and lung tissue of HS rats were harvested. (b) Representative micrographs for H&E staining of lung sections from each group. (c) Immunofluorescence micrographs of ROS expression (Red) of rat lungs from each group. (d) Protein expression of Nrf2 and GPX4 in lungs obtained from HS rats treated with hPMSC-Exos, hPMSC-Exos + DMSO, and ML385 + hPMSC-Exos (n=3 or n=4). (e)-(f) Quantitative analysis of western blot. Data are expressed as mean ± SD, *$P < 0.05$, **$P < 0.01$. HPMSC-Exos: human placental mesenchymal stem-cell-derived exosomes; HS: hemorrhagic shock; Nrf2: Nuclear factor erythroid 2-related factor 2; GPX4: glutathione peroxidase 4; H&E: hematoxylin and eosin; ROS: reactive oxygen species; DMSO: dimethyl sulfoxide. SD: standard deviation.

4 Discussion

HS is the primary cause of mortality in surgical and trauma patients (Lozano et al., 2012). Severe HS frequently results in infection, sepsis, and organ failure (Kalff et al., 1999). In this study, we based our HS rat model on the methods delineated in our previous studies to simulate clinical "pre-hospital", "transport", and "post-hospital" stages (Lu et al., 2013). According to the rat total blood-volume formula (Lee and Blaufox, 1985), the blood loss for HS rats was close to 50% of total body blood volume. All HS rats survived through the designated observation time periods of 24 h and 72 h, which reflects the reliability of the HS model.

Previous studies have thoroughly examined the progression and management of ALI/ARDS, aiming to enhance patient survival rates (Hu et al., 2022). Nevertheless, the overall prognosis for human patients remains unpromising, and there is presently no specific pharmacological treatment available. Research indicates that transplantation of MSCs can markedly improve HS-induced ALI. Regarding the source of MSCs, hPMSCs have superior abilities in terms of proliferation, differentiation, and immunomodulation; they are easy to sample and are available from a wide range of sources (Mashouri, et al., 2019). Consequently, we selected hPMSCs as a therapeutic intervention for ALI in rats subjected to HS.

The results indicate that the quantity of hPMSCs in the lungs of the HS group was very low compared to the sham group. We propose three potential explanations for this. Firstly, due to the detrimental effects of HS on various organs in the body, a significant number of hPMSCs migrate to the lungs and other affected organs within 24 h after administration. In addition, HS leads to a significant reduction in the number of hPMSCs in the lungs 72 h after administration. Owing to the multi-organ damage induced by HS across the body, hPMSCs may engage in active migration in HS rats, specifically relocating from the lungs to other affected organs. In 2002, Saito et al. proposed for the first time that MSCs have "homing" ability in vivo (Saito et al., 2002). MSCs or their exosomes migrate to damaged areas of the body upon entry (Xu et al., 2020; Huang et al., 2021; Huang et al., 2022). Reports indicate that tissues at the injury site produce numerous signaling molecules, including chemokines, adhesion factors, and growth factors, to recruit MSCs to the area (Cui and Madeddu, 2011). Consequently, the presence of hPMSCs in the major organs of HS rats is likely a result of the widespread damage to multiple organs caused by HS. Our results suggest that the migratory potential of hPMSCs may be valuable for evaluating organ damage following HS.

Prior research indicates that transplantation of bone marrow-derived MSCs can reduce pulmonary inflammation in animal models of HS. This transplantation also helps to preserve the integrity of lung endothelial cells and decrease pulmonary vascular permeability, thereby alleviating ALI caused by HS (Pati, et al., 2011; Potter, et al., 2018; Barry, et al., 2022; Wu et al., 2022). Nevertheless, there is no evidence available regarding the therapeutic effects of MSCs in terms of inhibition of ferroptosis in HS-induced ALI. Our study shows that hPMSCs are able to reduce the intensity of ROS. ROS shows a strong correlation with the amount of free iron in the lungs (Quinlan et al., 2002). Iron overload can exacerbate the conversion of hydrogen peroxide to free radicals by the Fenton reaction, leading to increased cytotoxicity and facilitating development of ALI (Chabot et al., 1998; Dixon and Stockwell, 2014; Zhang et al., 2019). Additionally, transplantation of hPMSCs may successfully restore mitochondrial structure in AT2 cells, inhibit ferroptosis, and mitigate HS-induced ALI. Exosomes have been reported to play a critical role in regulating the metabolic functions of cells and tissues (Arabpour et al., 2021).

Our research clarifies that hPMSCs may activate the Nrf2/GPX4 signaling axis through exosomes, thereby improving HS-induced ALI. Previous research also suggests that activation of Nrf2 has a protective effect on ALI or pulmonary fibrosis (Zhang et al., 2018; Lei et al., 2021; Xu et al., 2022; Zhao et al., 2022). Recently, increasing evidence has shown that most MSCs-mediated beneficial effects can be attributed to the functions of released exosomes (Zhang et al., 2022; Shen et al., 2023). For instance, certain miRNAs, specifically miR21, miR125b, let7, and miR24, are highly present in MSCs (Jann et al., 2021; Ma et al., 2023). However, the miRNAs transported by MSCs from various sources exhibit significant variation, which poses a challenge in conducting direct comparisons. This variability also imposes some limitations on the study of MSC exosomes.

Hence, more dedication should be directed towards this area to identify and elucidate the active agent in exosomes as well as to explain the underlying process.

The applicability of this study is limited by the fact that although male SD rats were used to maintain experimental consistency, further investigation is required to confirm the therapeutic effect of hPMSCs on female SD rats. In addition, the precise components of hPMSC-Exos that activate Nrf2 remain undefined. We hope to perform high-throughput sequencing of hPMSC-Exos to identify RNA or proteins that can effectively activate Nrf2.

5 Conclusions

Following transplantation of hPMSCs into HS rats, these cells predominantly localize in the liver and lungs, with a significant reduction in the quantity of hPMSCs in the lungs observed within 72 h. ALI is clearly observed at 24 h and 72 h post-HS in rats. Transplantation of hPMSCs significantly mitigates ALI in HS rats, leading to a reduction in oxidative stress and the inhibition of ferroptosis. The therapeutic effect may result from hPMSCs activating the Nrf2/GPX4 pathway via exosomes, which inhibits ferroptosis in AT2 cells and improves HS-induced ALI. This study indicates the distribution characteristics of hPMSCs in vital organs of HS rats and their potential therapeutic effects on HS-induced ALI.

Data availability statement

The data during the current study are available from the corresponding author on reasonable request.

Acknowledgments

This work was supported by the National Key Research and Development Program of China (2023YFC3603100 and 2023YFC3603105), Jiangsu Province's Entrepreneurship and Innovation Doctoral Talent (JSSCBS0422), Young Elite Scientists Sponsorship Program by Jiangsu Association for Science and Technology (JSTJ-2025-812), the Changzhou City's Longcheng Talent Program - Young Scientific and Technological Sponsorship Program (CZTJ-2025-47), the Science and Technology Climbing Plan of Changzhou First People's Hospital (KY20252476), Changzhou City's Basic Research Program (CJ20240074) and the Scientific Research Project of Changzhou Longcheng Advanced Medical Program (KY20241899).

We thank Wen Fang (the First Affiliated Hospital, School of Medicine, Zhejiang University, Hangzhou, China) for providing assistance with language editing. We also thank Chenyu Yang in the Center of Cryo-Electron Microscopy (CCEM), Zhejiang University for her technical assistance on Transmission Electron Microscopy.

Author contributions

Shuai JIANG designed and conducted the in vitro and in vivo experiments, analyzed the data and wrote the manuscript. Qin ZHANG and Ping WANG conducted some of the in vitro and in vivo experiments. Mengxiao FENG and Congying SONG conducted in vivo experiments. Yuanqiang LU conceived and conducted the research. Yuanqiang LU have read and verified the underlying data. All authors read and approved the final version of the manuscript.

Compliance with ethics guidelines

Shuai JIANG, Qin ZHANG, Ping WANG, Mengxiao FENG, Congying SONG and Yuanqiang LU declare that they have no conflict of interest.

Human placenta tissues were obtained from donors with informed consent at the First Affiliated Hospital, College of Medicine, Zhejiang University, China. The protocol of human tissues and cells handling that was approved by the Research Ethics Committee of the First Affiliated Hospital (Reference No. 2013–272). All experiments were conducted using protocols approved by the Animal Care Ethics Committee of the First Affiliated Hospital, Zhejiang University (Reference No. 2023-84).

References

Arabpour M, Saghazadeh A, Rezaei N, 2021. Anti-inflammatory and m2 macrophage polarization-promoting effect of mesenchymal stem cell-derived exosomes. *Int Immunopharmacol*, 97:107823. https://doi.org/10.1016/j.intimp.2021.107823

Bao Z, Liu Y, Chen B, et al., 2021. Prokineticin-2 prevents neuronal cell deaths in a model of traumatic brain injury. *Nat Commun*, 12(1):4220. https://doi.org/10.1038/s41467-021-24469-y

Barrachina L, Cequier A, Romero A, et al., 2020. Allo-antibody production after intraarticular administration of mesenchymal stem cells (mscs) in an equine osteoarthritis model: Effect of repeated administration, msc inflammatory stimulation, and equine leukocyte antigen (ela) compatibility. *Stem Cell Res Ther*, 11(1):52. https://doi.org/10.1186/s13287-020-1571-8

Barry M, Trivedi A, Pathipati P, et al., 2022. Mesenchymal stem cell extracellular vesicles mitigate vascular permeability and injury in the small intestine and lung in a mouse model of hemorrhagic shock and trauma. *J Trauma Acute Care Surg*, 92(3):489-498. https://doi.org/10.1097/ta.0000000000003487

Cao H, Yang J, Yu J, et al., 2012. Therapeutic potential of transplanted placental mesenchymal stem cells in treating chinese miniature pigs with acute liver failure. *BMC Med*, 10:56. https://doi.org/10.1186/1741-7015-10-56

Chabot F, Mitchell JA, Gutteridge JM, et al., 1998. Reactive oxygen species in acute lung injury. *Eur Respir J*, 11(3):745-757.

Cui Y, Madeddu P, 2011. The role of chemokines, cytokines and adhesion molecules in stem cell trafficking and homing. *Curr Pharm Des*, 17(30):3271-3279. https://doi.org/10.2174/138161211797904109

Di A, Mehta D, Malik AB, 2016. Ros-activated calcium signaling mechanisms regulating endothelial barrier function. *Cell Calcium*, 60(3):163-171. https://doi.org/10.1016/j.ceca.2016.02.002

Dixon SJ, Lemberg KM, Lamprecht MR, et al., 2012. Ferroptosis: An iron-dependent form of nonapoptotic cell death. *Cell*, 149(5):1060-1072. https://doi.org/10.1016/j.cell.2012.03.042

Dixon SJ, Stockwell BR, 2014. The role of iron and reactive oxygen species in cell death. *Nat Chem Biol*, 10(1):9-17. https://doi.org/10.1038/nchembio.1416

Dodson M, Castro-Portuguez R, Zhang DD, 2019a. Nrf2 plays a critical role in mitigating lipid peroxidation and ferroptosis. *Redox Biol*, 23:101107. https://doi.org/10.1016/j.redox.2019.101107

Dodson M, De La Vega MR, Cholanians AB, et al., 2019b. Modulating nrf2 in disease: Timing is everything. *Annu Rev Pharmacol Toxicol*, 59:555-575. https://doi.org/10.1146/annurev-pharmtox-010818-021856

Fan E, Dowdy DW, Colantuoni E, et al., 2014. Physical complications in acute lung injury survivors: A two-year longitudinal prospective study. *Crit Care Med*, 42(4):849-859. https://doi.org/10.1097/ccm.0000000000000040

Fu XR, Liu G, Halim A, et al., 2019. Mesenchymal stem cell migration and tissue repair. *Cells*, 8(8):18. https://doi.org/10.3390/cells8080784

Gore AV, Bible LE, Livingston DH, et al., 2016. Mesenchymal stem cells enhance lung recovery after injury, shock, and chronic stress. *Surgery*, 159(5):1430-1435. https://doi.org/10.1016/j.surg.2015.12.006

He YQ, Zhou CC, Yu LY, et al., 2021. Natural product derived phytochemicals in managing acute lung injury by multiple mechanisms. *Pharmacol Res*, 163:105224. https://doi.org/10.1016/j.phrs.2020.105224

Herridge MS, Tansey CM, Matté A, et al., 2011. Functional disability 5 years after acute respiratory distress syndrome. *N Engl J Med*, 364(14):1293-1304. https://doi.org/10.1056/NEJMoa1011802

Hu Q, Zhang S, Yang Y, et al., 2022. Extracellular vesicles in the pathogenesis and treatment of acute lung injury. *Mil Med Res*, 9(1):61. https://doi.org/10.1186/s40779-022-00417-9

Huang J, Zhang W, Yu J, et al., 2022. Human amniotic mesenchymal stem cells combined with ppcng facilitate injured endometrial regeneration. *Stem Cell Res Ther*, 13(1):17. https://doi.org/10.1186/s13287-021-02682-2

Huang Q, Cheng X, Luo C, et al., 2021. Placental chorionic plate-derived mesenchymal stem cells ameliorate severe acute pancreatitis by regulating macrophage polarization via secreting tsg-6. *Stem Cell Res Ther*, 12(1):337. https://doi.org/10.1186/s13287-021-02411-9

Jann JC, Mossner M, Riabov V, et al., 2021. Bone marrow derived stromal cells from myelodysplastic syndromes are altered but not clonally mutated in vivo. *Nat Commun*, 12(1):6170. https://doi.org/10.1038/s41467-021-26424-3

Kalff JC, Hierholzer C, Tsukada K, et al., 1999. Hemorrhagic shock results in intestinal muscularis intercellular adhesion molecule (icam-1) expression, neutrophil infiltration, and smooth muscle dysfunction. *Arch Orthop Trauma Surg*, 119(1-2):89-93. https://doi.org/10.1007/s004020050363

Lee HB, Blaufox MD, 1985. Blood volume in the rat. *J Nucl Med*, 26(1):72-76.

Lei L, Guo Y, Lin J, et al., 2021. Inhibition of endotoxin-induced acute lung injury in rats by bone marrow-derived mesenchymal stem cells: Role of nrf2/ho-1 signal axis in inhibition of nlrp3 activation. *Biochem Biophys Res Commun*, 551:7-13. https://doi.org/10.1016/j.bbrc.2021.03.009

Leung CH, Caldarone CA, Guan R, et al., 2019. Nuclear factor (erythroid-derived 2)-like 2 regulates the hepatoprotective effects of remote ischemic conditioning in hemorrhagic shock. *Antioxid Redox Signal*, 30(14):1760-1773. https://doi.org/10.1089/ars.2018.7541

Lozano R, Naghavi M, Foreman K, et al., 2012. Global and regional mortality from 235 causes of death for 20 age groups in 1990 and 2010: A systematic analysis for the global burden of disease study 2010. *Lancet*, 380(9859):2095-2128. https://doi.org/10.1016/s0140-6736(12)61728-0

Lu YQ, Gu LH, Zhang Q, et al., 2013. Hypertonic saline resuscitation contributes to early accumulation of circulating myeloid-derived suppressor cells in a rat model of hemorrhagic shock. *Chin Med J (Engl)*, 126(7):1317-1322.

Ma C, Qi X, Wei YF, et al., 2023. Amelioration of ligamentum flavum hypertrophy using umbilical cord mesenchymal stromal cell-derived extracellular vesicles. *Bioact Mater*, 19:139-154. https://doi.org/10.1016/j.bioactmat.2022.03.042

Maier RV, 2014. Scudder oration on trauma. A century of evolution in trauma resuscitation. *J Am Coll Surg*, 219(3):335-345. https://doi.org/10.1016/j.jamcollsurg.2014.04.011

Mashouri L, Yousefi H, Aref AR, et al., 2019. Exosomes: Composition, biogenesis, and mechanisms in cancer metastasis and drug resistance. *Mol Cancer*, 18(1):75. https://doi.org/10.1186/s12943-019-0991-5

Pati S, Gerber MH, Menge TD, et al., 2011. Bone marrow derived mesenchymal stem cells inhibit inflammation and preserve vascular endothelial integrity in the lungs after hemorrhagic shock. *PLoS One*, 6(9):e25171. https://doi.org/10.1371/journal.pone.0025171

Potter DR, Miyazawa BY, Gibb SL, et al., 2018. Mesenchymal stem cell-derived extracellular vesicles attenuate pulmonary vascular permeability and lung injury induced by hemorrhagic shock and trauma. *J Trauma Acute Care Surg*, 84(2):245-256. https://doi.org/10.1097/ta.0000000000001744

Quinlan GJ, Evans TW, Gutteridge JM, 2002. Iron and the redox status of the lungs. *Free Radic Biol Med*, 33(10):1306-1313. https://doi.org/10.1016/s0891-5849(02)00903-6

Saito T, Kuang JQ, Bittira B, et al., 2002. Xenotransplant cardiac chimera: Immune tolerance of adult stem cells. *Ann Thorac Surg*, 74(1):19-24; discussion 24. https://doi.org/10.1016/s0003-4975(02)03591-9

Shen K, Wang X, Wang Y, et al., 2023. Mir-125b-5p in adipose derived stem cells exosome alleviates pulmonary microvascular endothelial cells ferroptosis via keap1/nrf2/gpx4 in sepsis lung injury. *Redox Biol*, 62:102655. https://doi.org/10.1016/j.redox.2023.102655

Stockwell BR, 2022. Ferroptosis turns 10: Emerging mechanisms, physiological functions, and therapeutic applications. *Cell*, 185(14):2401-2421. https://doi.org/10.1016/j.cell.2022.06.003

Tasoulis MK, Livaditi O, Stamatakos M, et al., 2009. High concentrations of reactive oxygen species in the bal fluid are correlated with lung injury in rabbits after hemorrhagic shock and resuscitation. *Tohoku J Exp Med*, 219(3):193-199. https://doi.org/10.1620/tjem.219.193

Villar J, Fernández RL, Ambrós A, et al., 2015. A clinical classification of the acute respiratory distress syndrome for predicting outcome and guiding medical therapy*. *Crit Care Med*, 43(2):346-353. https://doi.org/10.1097/ccm.0000000000000703

Wang X, Shi W, Li M, et al., 2024. Rsl3 sensitizes glioma cells to ionizing radiation by suppressing tgm2-dependent DNA damage repair and epithelial-mesenchymal transition. *Redox Biol*, 78:103438. https://doi.org/10.1016/j.redox.2024.103438

Wang Y, Dong Z, Zhang Z, et al., 2022. Postconditioning with irisin attenuates lung ischemia/reperfusion injury by suppressing ferroptosis via induction of the nrf2/ho-1 signal axis. *Oxid Med Cell Longev*, 2022:9911167. https://doi.org/10.1155/2022/9911167

Wang Z, Chang P, Ye J, et al., 2021. Genome-wide landscape of mrnas, micrornas, lncrnas, and circrnas in hemorrhagic shock-induced ali/ards in rats. *J Trauma Acute Care Surg*, 90(5):827-837. https://doi.org/10.1097/TA.0000000000003119

Wu X, Darlington DN, Christy BA, et al., 2022. Intravenous administration of mesenchymal stromal cells leads to a dose-dependent coagulopathy and is unable to attenuate acute traumatic coagulopathy in rats. *J Trauma Acute Care Surg*, 92(3):542-552. https://doi.org/10.1097/ta.0000000000003476

Xu L, Zhu Y, Li C, et al., 2022. Small extracellular vesicles derived from nrf2-overexpressing human amniotic mesenchymal stem cells protect against lipopolysaccharide-induced acute lung injury by inhibiting nlrp3. *Biol Direct*, 17(1):35. https://doi.org/10.1186/s13062-022-00351-9

Xu R, Bai Y, Min S, et al., 2020. In vivo monitoring and assessment of exogenous mesenchymal stem

cell-derived exosomes in mice with ischemic stroke by molecular imaging. *Int J Nanomedicine*, 15:9011-9023. https://doi.org/10.2147/ijn.S271519

Yao F, Lu YQ, Jiang JK, et al., 2017. Immune recovery after fluid resuscitation in rats with severe hemorrhagic shock. *J Zhejiang Univ Sci B*, 18(5):402-409. https://doi.org/10.1631/jzus.B1600370

Zhang K, Jin Y, Lai D, et al., 2020. Rage-induced ilc2 expansion in acute lung injury due to haemorrhagic shock. *Thorax*, 75(3):209-219. https://doi.org/10.1136/thoraxjnl-2019-213613

Zhang S, Jiang W, Ma L, et al., 2018. Nrf2 transfection enhances the efficacy of human amniotic mesenchymal stem cells to repair lung injury induced by lipopolysaccharide. *J Cell Biochem*, 119(2):1627-1636. https://doi.org/10.1002/jcb.26322

Zhang V, Nemeth E, Kim A, 2019. Iron in lung pathology. *Pharmaceuticals (Basel)*, 12(1) https://doi.org/10.3390/ph12010030

Zhang Y, Yang S, Qiu Z, et al., 2022. Pyrogallol enhances therapeutic effect of human umbilical cord mesenchymal stem cells against lps-mediated inflammation and lung injury via activation of nrf2/ho-1 signaling. *Free Radic Biol Med*, 191:66-81. https://doi.org/10.1016/j.freeradbiomed.2022.08.030

Zhao R, Wang L, Wang T, et al., 2022. Inhalation of msc-evs is a noninvasive strategy for ameliorating acute lung injury. *J Control Release*, 345:214-230. https://doi.org/10.1016/j.jconrel.2022.03.025

Zhou Y, Li P, Goodwin AJ, et al., 2019. Exosomes from endothelial progenitor cells improve outcomes of the lipopolysaccharide-induced acute lung injury. *Crit Care*, 23(1):44. https://doi.org/10.1186/s13054-019-2339-3